

Nexus sine qua non: Essentially connected neural networks for spatial-temporal forecasting of multivariate time series

Tong Nie¹, Guoyang Qin¹, Yunpeng Wang², Jian Sun^{1*}

¹ Department of Traffic Engineering & Key Laboratory of Road and Traffic Engineering, Ministry of Education, Tongji University, Shanghai 201804, China,

² Beijing Key Laboratory for Cooperative Vehicle Infrastructure Systems and Safety Control, School of Transportation Science and Engineering, Beihang University, Beijing 100191, China,

nietong@tongji.edu.cn, 2015qgy@tongji.edu.cn,
ypwang@buaa.edu.cn, sunjian@tongji.edu.cn

Abstract

Modeling and forecasting multivariate time series not only facilitates the decision making of practitioners, but also deepens our scientific understanding of the underlying dynamical systems. Spatial-temporal graph neural networks (STGNNs) are emerged as powerful predictors and have become the de facto models for learning spatiotemporal representations in recent years. However, existing architectures of STGNNs tend to be complicated by stacking a series of fancy layers. The designed models could be either redundant or enigmatic, which pose great challenges on their complexity and scalability. Such concerns prompt us to re-examine the designs of modern STGNNs and identify core principles that contribute to a powerful and efficient neural predictor. Here we present a compact predictive model that is fully defined by a dense encoder-decoder and a message-passing layer, powered by node identifications, without any complex sequential modules, e.g., TCNs, RNNs, and Transformers. Empirical results demonstrate how a simple and elegant model with proper inductive basis can compare favorably w.r.t. the state of the art with elaborate designs, while being much more interpretable and computationally efficient for spatial-temporal forecasting problem. We hope our findings would open new horizons for future studies to revisit the design of more concise neural forecasting architectures. **PyTorch implementations and reproducible results are publicly available at: [code]**¹.

1 Introduction

Forecasting future time series is one of the most popular applications of modern deep spatial-temporal models [1, 2, 3, 4, 5, 6]. Spatial-temporal multivariate time series forecasting (STMF) has already driven tremendous achievements in a diverse array of applications, such as traffic flow modeling [2], weather prediction [7], energy management [8], etc. A plethora of works have devoted to elaborate advanced deep neural network models to capture the entangled correlations in spatiotemporal data. Having been examined by massive literature, spatial-temporal graph neural networks (STGNNs) are supposed to be the de facto standard on this challenging task and has attracted particular interests.

Preprint.

¹Source code will be open-sourced upon publication

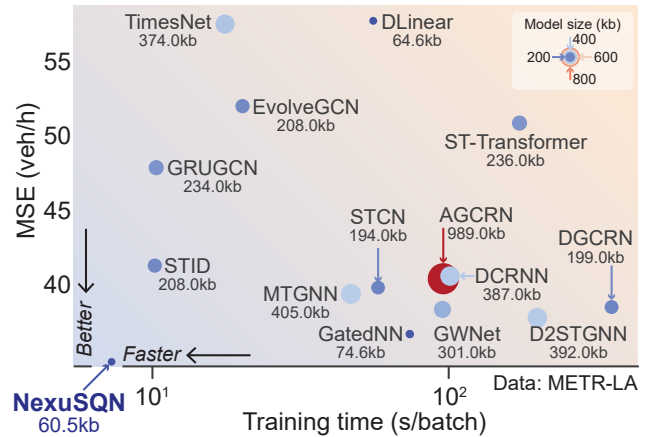


Figure 1: This figure compares the forecasting performance of our model, NexuSQN, with 14 modern neural architectures on the well-known METR-LA benchmark. Our model outperforms the others in terms of training time, Mean Squared Error (MSE), and model size.

Particularly, stacking multiple well-designed spatial-temporal blocks or layers (usually consist of graph neural networks, sequential networks, and additional components) in turn tend to be a standardized practice in newly-emerged STGNNs. Despite promising results on testing datasets, such manners often produce overly cumbersome and intricate architectures, hindering the understanding of their behaviors and the discovery of components that really contribute to the forecasting. It is dubious that the design of some advanced STGNNs might conceptually complicate the forecasting process and make the model prone to over-fit the training data and non-trivial to implement, thereby weakening the generalization ability. While popular sequential models like recurrent neural networks (RNN), temporal convolution networks (TCN), WaveNet, and Transformers are theoretically well-posed for series modeling and become the indispensable components of the majority of existing works in this line of research [9], few of studies validate whether they are truly effective and indispensable for STMF under

the spatiotemporal settings. The above phenomena prompt us to revisit the design of STGNNs and endeavor to answer the intriguing question: **what kind of STGNNs do we really need for STMF?**

Encouragingly, recent works have revisited the design of neural forecaster and look back to develop simpler model architectures for long-term time series forecasting (LTSF) problems [10, 11, 12, 13, 14] and empirically show the superiority of simple designs over their complex counterparts. While, investigation into short-term STMF task is still lacked. Different from LTSF, the studied STMF is more challenging in two ways: ① more complex temporal patterns (e.g., nonstationary) with high resolution; ② subtle interaction between different series (locations). Therefore, we conjecture that the emerging Transformers-like or simpler linear models designed for LTSF are less effective in the context of spatiotemporal data, as the above methods basically adopt a channel-independence assumption and ignore the explicit correlations between series [10, 12]. Although a pioneering work [15] demonstrated a competitive baseline with simple multi-layer perceptrons (MLPs) and identity information, the limited expressive capacity undermines their utility in more complex scenarios.

Motivated by these research gaps, we attempt to go beyond such acknowledged paradigms and question the necessity and validity of using complex STGNNs for STMF. Through careful inspection, we find the technical complexities of current STGNNs lie in the following three aspects:

- Complicated sequential encoder and decoder, e.g., self-attention mechanism and casual convolutions;
- Intricate graph learning module, e.g., all pair-wise interactions of raw or transformed features;
- Expensive and stacked graph convolution layers, e.g., graph attention or graph transformers.

In contrast, we explore how a concise and simple model can perform comparatively with its complicated counterparts while enjoying much faster training, less computational complexity, fewer model hyper-parameters, and easier implementations (see Fig. 1). Concretely, Our simplified model features three basic components: ① A dense *MLP-encoder* with folded series as inputs; ② A *parameter-efficient message-passing backbone* with node identity for abstracting low-frequency representations; ③ A dense *MLP-readout* for direct multi-step forecasting. Empirical results on some common benchmark datasets indicate an embarrassing but intriguing fact that neither of these complicated modeling techniques is always essential for STMF. The main novelty and contributions of our work are three-fold:

- We demonstrate a conceptually and technically simple neural forecasting architecture by replacing redundant components with essentially connected blocks;
- We identify and highlight the significance of node identity in STGNNs, including parameter customization, positional representation, and structural representation;
- We conduct extensive experiments to evaluate the performance of the proposed model on 8 common benchmark datasets and reveal its superiority by comparing with more than 10 state-of-the-art deep learning models.

We hope our results can encourage further works on this topic to go beyond the sphere of complex STGNNs and reconsider the significance of simpler models. As we aim to grasp the most essential components and present a domain-agnostic method for general STMF tasks, we refer to our model as *Nexus Sine Qua Non* (NexuSQN) networks.

2 Notations and Preliminaries

This work considers multivariate time series prediction problem under the spatiotemporal background. To ease of representation, we follow the terminology of previous works [16, 17]. Particularly, N time series are collected from different geographic locations and each of them owns a d_{in} -dimensional records, denoted by $\mathbf{x}_t^i \in \mathbb{R}^{d_{in}}$. The whole measurement at time t can be linked by the physical or internal connections between series and forms a graph signal matrix $\mathbf{X}_t \in \mathbb{R}^{N \times d_{in}}$ with side information represented by the static (possibly time-varying) adjacent matrix $\mathbf{A} \in \mathbb{R}^{N \times N}$. In addition, we indicate with the tensor $\mathcal{X}_{t:t+T} \in \mathbb{R}^{N \times T \times d_{in}}$ the graph signal sequence within time interval $[t, t+T)$. For STMF dataset, exogenous variables about periodicity and seasonality are readily collected at each time step, which is denoted by $\mathbf{U}_t \in \mathbb{R}^{N \times d_u}$. Similarly, node-specific features like positional encoding is indicated as $\mathbf{V} \in \mathbb{R}^{N \times d_v}$. Combining the above components, the input graph signals within a historical time window w can be denoted as $\mathcal{G}_{T-w:T} = \langle \mathcal{X}_{T-w:T}, \{\mathbf{U}_t, \mathbf{V}, \mathbf{A}_t, t = T-w, \dots, T\} \rangle$. The objective of STMF is to forecast the next H horizons of graph signals given a window of W historical records with a predictive function $F_\theta(\cdot)$:

$$\widehat{\mathcal{G}}_{T+1:T+H} = F_\theta(\mathcal{G}_{T-W:T}), \quad (1)$$

where θ is the model parameters to be learned.

3 Rethinking the Mechanism of STGNNs

This section briefly discusses the archetypes and forecasting mechanisms of modern STGNNs. Through revisiting different branches of related research on broader horizons, we identify key principles for designing powerful STGNNs.

Architecture templates of STGNNs Following the terminology in [18, 19], we can categorize common STGNNs into (1) *time-and-graph (T&G)* networks and (2) *Time-then-graph (TTG)* models, conditioning on whether the temporal encoders and spatial encoders are stacked alternately or sequentially. The former are the most widely used ones in STMF, e.g., [20, 2, 3, 21], which can be described as:

$$\begin{aligned} \mathbf{H}_{t-W:t}^{(l)} &= \text{ENCODER}(\mathbf{H}_{t-W:t}^{(l-1)}), \quad l \in \{1, \dots, L\} \\ \widehat{\mathbf{H}}_\tau^{(l)} &= \text{MPBLOCK}(\mathbf{H}_\tau^{(l)}, \mathbf{A}), \quad \tau \in \{t-W, \dots, t\} \\ \widehat{\mathbf{X}}_{t:t+H} &= \text{DECODER}(\widehat{\mathbf{H}}_{t-W:t}^{(L)}), \end{aligned} \quad (2)$$

while, TTG is developed recently which follows a more compact format that process series and graph information

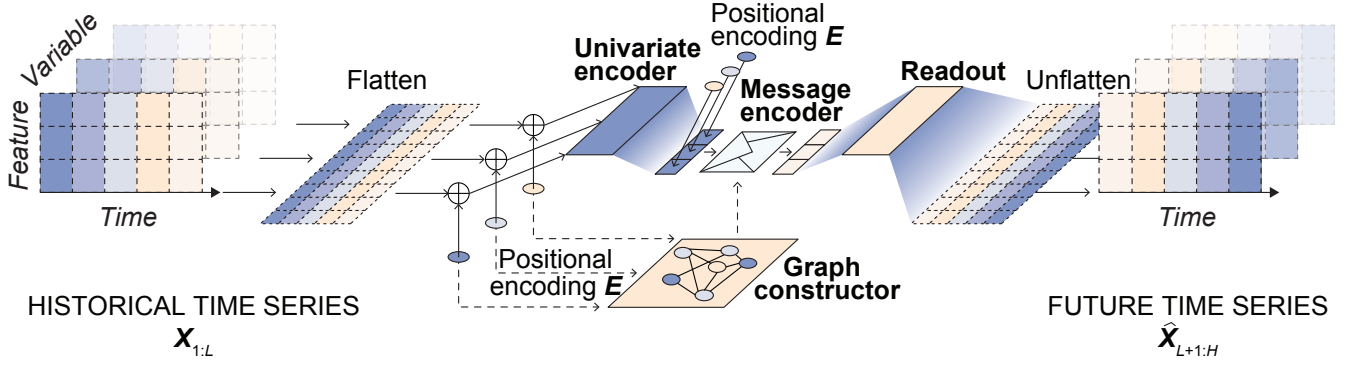


Figure 2: Overview architecture of the proposed NexuSQN predictor. Input time series are folded and fed to a univariate MLP encoder, then pass through a graph mixer consists of a parameter-efficient message-passing operator. Then a final MLP readout produces multi-step predictions. The node positional encoding E closely connects each component.

sequentially with fewer temporal encoders [22]:

$$\begin{aligned} \mathbf{H}_t^0 &= \text{ENCODER}(\mathbf{X}_{t-W:t}), \\ \mathbf{H}_t^{(l)} &= \text{MPBLOCK}(\mathbf{H}_t^{(l-1)}, \mathbf{A}), l \in \{1, \dots, L\} \quad (3) \\ \mathbf{X}_{t:t+H} &= \text{DECODER}(\mathbf{H}_t^{(L)}), \end{aligned}$$

where $\text{ENCODER}(\cdot)$ denotes a temporal encoder to process time series features, $\text{DECODER}(\cdot)$ is a task-specific readout layer to perform predictions, and the core $\text{MPBLOCK}(\cdot)$ layers consist of several stacked message-passing (graph convolutions) layers to aggregate information on the given graph \mathcal{G} . Since the expensive message-passing is carried out at each time step in T&G, and the encoding process is usually repeated several times, TTG is demonstrated to be more efficient and expressive than T&G under certain settings [18].

Message-passing operation of STGNNs The message-passing (MP) operator in Eq. 3 is at the core of TTG models. Kindly note that we use MP and graph convolution interchangeably throughout this paper. GNNs can be considered as a general model of message-passing neural networks (MPNN) [23]. A complete MPNN contains three forward computation phases and a final output function: message passing, feature aggregation, node updating, and readout layer, parameterized by a message function, update function, and a readout function respectively. Under the spatiotemporal settings, MPNN can be formulated as follows by omitting the readout operation:

$$\begin{aligned} \mathbf{m}_t^{i \leftarrow j, (l)} &= \text{MSG}_l(\mathbf{h}_t^{i, (l-1)}, \mathbf{h}_t^{j, (l-1)}, e_{i \leftarrow j}^t), \\ \mathbf{m}_t^{i, (l)} &= \text{AGG}(\mathbf{m}_t^{i \leftarrow j, (l)}; \forall j \in \mathcal{N}(i)), \quad (4) \\ \mathbf{h}_t^{i, (l)} &= \text{UP}_l(\mathbf{h}_t^{i, (l-1)}, \mathbf{m}_t^{i, (l)}), \end{aligned}$$

where $e_{i \leftarrow j}^t$ is the edge weight between node i and j at time t , MSG , AGG and UP are message, aggregation, and updating functions. Eq. 4 is conducted in parallel for all nodes at each time step. The aggregation and message function is usually permutation invariant. For simplicity, we instantiate the aggregation function with a simple summation and the

message function with a MLP. In addition, the edge weights in MSG can either be pre-defined or learned from data.

Forecasting mechanism of neural predictors Following the discussions in [10, 13], we can split the deep forecasting models into two categories according to their encoding mechanisms: (1) time-dependent, and (2) data-dependent. Concretely, a simple linear encoder can be expressed as follows:

$$\mathbf{h}_{t+1:t+H} = \mathbf{W}\mathbf{h}_{t-W:t} + \mathbf{b}, \quad (5)$$

which forms a vanilla autoregressive model at each forecasting horizon:

$$h_{t+h} = \sum_{k=0}^W w_k^h h_{t-k} + b_k, h \in \{1, \dots, H\}. \quad (6)$$

For a specific forecasting horizon, its regression weights solely condition on the relative location in the historical series and remain unchanged for input sequence at different times. Conversely, the behaviors of RNNs-like and Transformers-like encoders are data-dependent:

$$h_{t+h} = \sum_{k=0}^W \mathcal{F}_k(\mathbf{h}_{t-W:t}) h_{t-k} + b_k, h \in \{1, \dots, H\}, \quad (7)$$

where $\mathcal{F}_k(\cdot)$ is a data-driven function, e.g., self-attention. We claim that this format follows a fully time-varying autoregressive process [24] that the autoregressive process are parameterized by dynamically changing coefficients over time. This over-parameterized settings are prone to overfit the data rather than capturing the temporal relations like position and order or series [10].

Global and local perspectives Depending on whether the parameters are set globally or locally and how the relationships between series are processed, STGNNs have different ways to deal with multivariate time series [25, 17, 12]. Taking encoder only for example, there are three modes: ① Global univariate model: each series is processed independently by a shared model that is jointly trained on the whole

dataset [10, 26]; ② Local univariate model: each time series has a own encoder that is trained based on itself solely [27]; ③ Multivariate model: predictions of all series are made simultaneously by explicitly modeling the interaction between them.

Most of the well-known STGNNs belongs to the category of *global-multivariate* models, i.e., all nodes share a univariate encoder (e.g., RNNs) and multivariate extensions (e.g., GNNs), which can be formally given as:

$$\widehat{\mathbf{X}}_{t+1:t+H} = F_G(\mathcal{G}_{t-W:t}|\theta), \quad (8)$$

where θ indicates the model parameters. Two apparent superiority of global-multivariate models are the exploitation of relational information and fewer model parameters.

To take into account the series-specific *local* dynamics, ones can specialize the global models with customized local encoder for each item. One straightforward way is to develop a univariate model for each time series, i.e.,

$$\hat{\mathbf{x}}_{t+1:t+H}^i = f_i(\mathbf{x}_{t-W:t}^i|\theta^i), \quad (9)$$

where $f_i(\cdot|\theta^i)$ is the parameterized model for i -th time series (node). Local models benefit the adaption of distributions of individual series. However, such realization is susceptible to over-fitting and usually hard to optimize due to the large parameter space.

A more feasible choice is to integrate local models with global ones (global-local), followed the encoder-decoder paradigm [22]:

$$\begin{aligned} \mathbf{h}_t^i &= \text{ENCODER}_i(\mathbf{x}_{t-W:t}^i|\theta^i), \\ \widehat{\mathbf{H}}_t &= F_G([\mathbf{h}_t^1|\mathbf{h}_t^2 \dots |\mathbf{h}_t^n]|\Phi), \\ \hat{\mathbf{x}}_{t:t+H}^i &= \text{DECODER}_i(\widehat{\mathbf{h}}_t^i|\psi^i), \end{aligned} \quad (10)$$

where θ^i, ψ^i and Φ are parameters of univariate local encoder, decoder and multivariate global model, respectively. In this formulation, F_G can be arbitrary multivariate extensions that extract relational representations.

Overall, we prefer a multivariate TTG model that enjoys both the global-local and time-dependent patterns, which we regard as the cornerstone of an efficient neural predictor.

4 Essentially Connected Neural Predictors

This section elaborates our simplified model for STMF based on the above discussions. Fig. 2 presents the overall neural architecture. The rationales of our model are the flexible usage of positional encoding, and the simplicity of each modular design. Particularly, our model features a essentially-connected TTG architecture based on a message-passing backbone. Three basic principles are discovered for designing an efficient spatiotemporal predictor: (1) dense and localized univariate series encoder, (2) multivariate relational graph mixer, and (3) direct multi-step readout.

We cast the STMF into a node regression problem and depend on simple message aggregation with node identification to learn spatiotemporal representations, dispensing with complex temporal models (e.g., RNNs, Self-attention, and TCNs) entirely. By developing a concise and comprehensible neural predictor, we endeavor to empirically answer the following key questions with regard to STMF:

- Q1** Are complex sequential techniques always necessary?
- Q2** How to efficiently model relations between series?
- Q3** How powerful are node identification in STMF?

With these questions, we provide detailed descriptions about each modular component in the following sections.

4.1 UNIVARIATE DENSE SERIES ENCODER AND DECODER

Having inspected the necessity of complex sequential models, we propose to design a conceptually and technically simpler encoder-decoder architecture.

Temporal encoder for flattened series Most existing STGNNs handle the time and feature dimension separately, i.e., first projecting the input features at each time step to high-dimensional representations independently, and correlates different time steps with sequential models like RNNs. Despite reasonable and intuitive, this treatment increases the model complexity and the risk of overfitting significantly, especially when hidden dimension is much larger than channel (feature) dimensions.

As such, we proposed to flatten raw time series along time dimension and instantiate the temporal encoder in Eq. 3 with a simple MLP layer:

$$\begin{aligned} \mathbf{X}_{t-W:t} &= \text{FOLD}([\mathcal{X}_{t-W:t}|\mathbf{U}_t], \text{dim} = 0), \\ \mathbf{H}^0 &= \text{MLP}(\mathbf{X}_{t-W:t}), \end{aligned} \quad (11)$$

where $\text{FOLD}(\cdot) : \mathbb{R}^{N \times T \times d_{in}} \rightarrow \mathbb{R}^{N \times T d_{in}}$ is the flattening operation. By flattening the time dimension, the temporal information of entire time series is stored in the hidden state \mathbf{H}^0 , which implicitly models the temporal correlations. We inject series PE here to inform the temporal encoder with time series information, e.g, periodicity and seasonality.

Multi-step forecasting with simple readout The last component for a neural predictor is a task-specific readout (output) layer. For multi-step STMF, we adopt a simple decoder with a MLP and reshaping layer:

$$\begin{aligned} \widehat{\mathbf{X}}_t &= \text{MLP}(\mathbf{H}_t^{(L)}), \\ \widehat{\mathcal{X}}_{t:t+H} &= \text{UNFOLD}(\widehat{\mathbf{X}}_t), \end{aligned} \quad (12)$$

where $\text{UNFOLD}(\cdot)$ is the inverse linear operator of $\text{FOLD}(\cdot)$. We do not use STPE in the decoder since we found it benefits marginally to the final performance. Again, we do not elaborate a complex sequential decoder and the multi-step predictions are regressed directly.

4.2 VERSATILITY OF SPATIAL-TEMPORAL IDENTIFICATIONS

One cornerstone of the proposed framework is the versatile positional encoding (PE). In the context of GNNs' representation ability [28], the roles of node positional encoding in our model are threefold, including: *parameter customization, positional representation, and structural representation*.

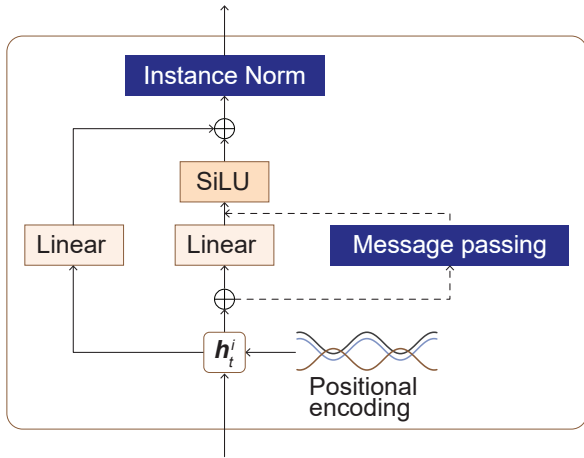


Figure 3: Basic modular block of our model. The message-passing step is optional depending on whether structural information is desirable.

Spatial-temporal positional encoding Following the original design of Transformer model [29], we adopt sinusoidal PE $\mathbf{U}_t \in \mathbb{R}^{T \times d_s}$ to inject the time-of-day information of each time series along time dimension.

For space (graph) dimension, we consider setting a unique identifier for each series. One optional PE is structural embedding, e.g., random-walk diffusion matrix [30]. For simplicity, we use learnable node embedding as a simple index PE without any structural priors. Specifically, we assign learnable vectors with random initialization for all series, denoted as $\mathbf{E} \in \mathbb{R}^{N \times d_{\text{emb}}}$, then it is included into the forward computation as endogenous variables and its gradient is updated end-to-end by back propagation.

Such a node embedding (or PE) reflects the static features of each node, e.g., dominating traffic pattern of a sensor, and it is agnostic to time information. Inspired by [31], we propose to inform the PE with temporal information, like periodicity and seasonality. Given $\mathbf{U}_t \in \mathbb{R}^{T \times d_s}$, we first fold the time dimension and project it into the hidden space:

$$\begin{aligned} \tilde{\mathbf{u}} &= \mathbf{W}_U \text{FOLD}(\mathbf{U}_t), \\ \tilde{\mathbf{U}} &= \text{BROADCAST}(\tilde{\mathbf{u}}, N), \\ \mathbf{E}_t &= \text{RESMLP}(\text{RESMLP}(\mathbf{E} + \tilde{\mathbf{U}})), \end{aligned} \quad (13)$$

where $\mathbf{W}_U \in \mathbb{R}^{d_{\text{emb}} \times T d_s}$ is learnable weights, and $\text{BROADCAST}(\cdot)$ duplicates the inputs with given times along a new dimension. \mathbf{E}_t is the final spatiotemporal positional encoding (STPE). Since input data from different time-of-day intervals has different sinusoidal stamps, STPE can reflect periodicity of series.

Specialize equivalent local encoders As discussion in section 3, recent works have indicated the importance of considering *local* effects by assigning a specific encoder (decoder) for individual series [10, 13]. Despite promising improvements for series with significant periodic and seasonal patterns, it could lead to overwhelming parameter capacity

and overfit the training data when the temporal patterns are localized.

Instead, we consider an amortized specialization, i.e., adding learnable node embedding to each series to grasp node-specific local dynamics [17], which is equivalent to instantiate ENCODER_i in Eq. 10 with much fewer parameters:

$$\mathbf{h}_i^1 = \text{RESMLP}(\mathbf{h}_i^0 + \mathbf{e}_i), \quad (14)$$

where RESMLP are MLP with residual-connection [32]. We add the STPE to the node features directly, instead of concatenation, to reduce the number of parameters.

Discriminative node representations Since GNNs concentrate on local graph structures, one drawback of the widely-used GNNs is the inadequacy to differentiate two nodes with the same or close neighborhood structure [33, 34]. Under this circumstance, two nodes that are far apart on the graph could have similar features, thereby hindering the representation power of GNNs, which is understood as *spatial indistinguishability problem* [35].

We consider a lightweight but effective solution to mitigate this problem, i.e., to parameterize each node with a discriminative identifier before MP stage [36]. As the globally set embedding table \mathbf{E} is randomly sampled, we can directly incorporate it into the MP process:

$$\mathbf{m}_t^{i \leftarrow j} = \text{MSG} \left(\begin{bmatrix} \mathbf{h}_t^i \\ \mathbf{e}^i \end{bmatrix}, \begin{bmatrix} \mathbf{h}_t^j \\ \mathbf{e}^j \end{bmatrix}, e_{i \leftarrow j}^t \right). \quad (15)$$

Moreover, adding learnable features to each node high-frequency components to low-frequency node representations [37] to highlight the impact of local events in spatiotemporal data [35]

Learning latent relational graphs Most existing STGNNs depend on apriori knowledge about the dependency between different series, e.g., spatial proximity of different sensors [38]. Despite being widely used in modern forecasting tasks, pre-determined graphs could be biased and misleading. Moreover, the performance is sensitive to the hyper-parameters of graph constructors [19]. To this end, we conjecture that these exogenous features might not mirror the inherent relations of multivariate series and the pre-determined graphs are redundant for spatiotemporal data. With adequate historical records that contain rich relational information about the underlying interaction among series, latent graphs can be implicitly learned from data.

Srinivasan and Ribeiro [28] theoretically analyzed the equivalence between positional node embeddings and structural graph representations for GNNs. Inspired by their results, we consider a very simple realization of graph constructor (link predictor) directly using the STPE in Eq. 13:

$$\mathbf{A}_t = \text{SOFTMAX}(\mathbf{E}_t \cdot \mathbf{E}_t^T). \quad (16)$$

Note that since different time interval produces different temporal encoding, the generated adjacent matrix is time-varying within a period, e.g, a day. Compared with attention based graph learning method, e.g., graph attention [39],

fully-connected attention [5, 22], which entails the all pair-wise attendance of data (or features), the proposed method reduce the parameters to be estimated from N^2 to $d_{\text{emb}}N$ for inferring a dense and fully connected graph.

4.3 PARAMETER-EFFICIENT NEURAL MESSAGE PASSING

Recall that we have encoded the temporal information in \mathbf{H}^1 , no additional sequential models are required. We now focus on the formulation of global model in Eq. 10, i.e., the MPBLOCK. The basic forward computation of our model is illustrated in Fig. 3. Note that our method only propagates features in the MPBLOCK, rather than in each time step, which makes it more efficient than alternately stacked spatial-temporal blocks.

The workflow of MPNNs in Eq. 4 generally contains two stages: 1) message-passing (MP), and 2) feed-forwarding (FF) [40]. MP conducts feature aggregation, and FF performs feature transformation. As can be seen, what differentiates GNNs from MLPs is the MP step that aggregates neighborhood information on graphs. In this sense, we can formulate the following two types of encoders as the foundation of our framework:

$$\text{ENCODER - MSG : } \mathbf{H}^{(l)} = \sigma(\mathbf{f}(\mathbf{A})\mathbf{H}^{(l-1)}\mathbf{W}_{\text{MPNN}}^{(l)}), \quad (17)$$

$$\text{ENCODER - Dense : } \mathbf{H}^{(l)} = \sigma(\mathbf{H}^{(l-1)}\mathbf{W}_{\text{MLP}}^{(l)}),$$

where \mathbf{W}_{MPNN} and \mathbf{W}_{MLP} are trainable weights for MPNNs and MLPs respectively, $f(\cdot)$ is the function of relational graphs. Moreover, as empirically shown in [41, 42], both MPNNs and MLPs can share close feature spaces under certain conditions. This intuition enables us to formulate simpler models by narrowing the gap between MPNNs and MLPs.

Graph mixer for relations modeling The proposed parameter-efficient neural message-passing block can be viewed as a structured feature (channel) mixer, which is a special case of the MLP mixer in [13].

After omitting the bias, time series mixer in [13] can be formulate as:

$$\mathbf{H}^{(l)} = \sigma(\Theta_{\text{feature}}^{(l)}\mathbf{H}^{(l-1)}\Theta_{\text{time}}^{(l)}), \quad (18)$$

where Θ_{time} is the weight for time mixing and Θ_{feature} can be viewed as an unconstrained graph learning module and contains N^2 parameters. Instead, we adopt a structured MPNN as the graph (channel) mixer:

$$\text{MPNN}(\mathbf{H}, \mathbf{A}; \Theta) = \sigma(\mathbf{A}\mathbf{H}\Theta), \quad (19)$$

where \mathbf{A} is learned in Eq. 16. It can be seen that our graph mixer ensures the normalization of adjacent matrix and explicitly models the pair-wise interactions among nodes. By exploiting the relational information, our model achieves a modular extension from univariate models to multivariate.

Normalization and residual connection The technique of instance normalization has been adopted to mitigate distribution shift problem recently [43, 26]. From another perspective, Deng et al. [35] suggest that deep forecasting models could fail to discriminate temporal components with different frequency, and applying a temporal normalization can reinforce the representations of high-frequency parts.

To help the model better distinguish meaningful temporal components from the input series, we apply an instance normalization layer [44] in the encoder:

$$\tilde{h}_i^t = \frac{h_i^t - \mathbb{E}[h_i^t]}{\sqrt{\text{Var}[h_i^t] + \epsilon}}\gamma_i + \beta_i, \quad (20)$$

where γ and β are learnable parameters, and the expectation and variance are calculated per-dimension separately for each item in a mini-batch. Eq. 20 is equivalent to the temporal normalization in [35], so that the encoder can better exploit the high-frequency representations.

We also preserve a shortcut for the linear part in each block. When all the residual connections is activated (e.g., when relational information is unnecessary), our model can degenerate into a class of linear models with channel-independence, e.g., [10, 12], which show great potential for long-term series forecasting.

Smaller model size with parameter sharing Different from recent design trends that assign different node embedding or graphs for different layers [45, 46], we set the PE globally shared for all dense encoders, message-passing encoders as well as graph constructors. The consideration is to facilitate the end-to-end training of random node embedding and reduce model size.

In addition, recent works empirically show that MLPs and GNNs can share similar feature spaces [41, 42]. Without the MP operation, MPNNs can degenerate to MLPs. In light of this, we instantiate two consecutive MP layers with shared linear transform for FF.

In section 6, we will show that two layers of MPNN with dense graphs are adequate for capturing long range spatial dependency, with no need to stack multiple sparse graph aggregators. This observation is aligned with the recent results that the expressive power of GNNs are determined by both of the depth and width of models [33], and a single MP can gather adequate information from a large number of nodes when the underlying graph is dense [47].

5 Related Works

Spatiotemporal forecasting of multivariate time series has sparked great interests in both academia and industry. To exploit the relationship between different series, STGNNs take all series as inputs and leverage the message-passing mechanism of GNNs to correlate them. Then, the characteristics of time series are preserved by a well-defined temporal module. Following such paradigm, a vast array of studies have made remarkable achievements. Among these works, Yu et al. [1] alternatively conduct graph and temporal convolution to extract localized features. Li et al. [2] adopt diffusion graph convolution to enable the gated recurrent unit network aware of structural information. Wu et al. [3], Bai et al. [4] further reinforce the model capacity with graph learning techniques. Furthermore, attention mechanism is introduced into STGNNs to utilize pair-wise interaction between series both on space and time dimensions [48, 49, 50].

Research on simplified deep models for STMF has been relatively limited. Cini et al. [16] first proposed a pre-

	METR-LA						PEMS-BAY					
	15 min	30 min	60 min	Average			15 min	30 min	60 min	Average		
	MAE	MAE	MAE	MAE	MSE	MAPE (%)	MAE	MAE	MAE	MAE	MSE	MAPE (%)
AGCRN	2.85	3.19	3.56	3.14	40.94	8.69	1.38	1.69	1.94	1.63	13.59	3.71
DCRNN	2.81	3.23	3.75	3.20	41.12	8.90	1.37	1.72	2.09	1.67	14.52	3.78
Graph WaveNet	2.74	3.14	3.58	3.09	38.86	8.52	1.31	1.65	1.96	1.59	13.31	3.57
GatedGN	2.72	3.05	3.43	3.01	37.19	8.20	1.34	1.65	1.92	1.58	13.17	3.55
GRUGCN	2.93	3.47	4.24	3.46	48.47	9.85	1.39	1.81	2.30	1.77	16.70	4.03
EvolveGCN	3.27	3.82	4.59	3.81	52.64	10.56	1.53	2.00	2.53	1.95	18.98	4.43
ST-Transformer	2.97	3.53	4.34	3.52	51.49	10.06	1.39	1.81	2.29	1.77	17.01	4.09
STCN	2.84	3.25	3.80	3.23	40.34	9.02	1.37	1.71	2.08	1.66	14.11	3.75
STID	2.82	3.18	3.56	3.13	41.83	9.07	1.32	1.64	1.93	1.58	13.05	3.58
MTGNN	2.79	3.12	3.46	3.07	39.91	8.57	1.34	1.65	1.91	1.58	13.52	3.51
D2STGNN	2.74	3.08	3.47	3.05	38.30	8.44	1.30	1.60	1.89	1.55	12.94	3.50
DGCRN	2.73	3.10	3.54	3.07	39.02	8.39	1.33	1.65	1.95	1.59	13.12	3.61
DLinear	3.18	3.84	4.88	3.86	58.42	10.91	1.56	2.11	2.91	2.10	24.11	4.72
TimesNet	3.27	3.80	4.68	3.83	58.22	10.56	1.69	2.05	2.63	2.07	24.22	4.65
NexuSQN	2.65	2.99	3.37	2.95	35.31	8.05	1.30	1.60	1.87	1.54	12.35	3.46

Table 1: Results on benchmark traffic speed datasets. MAE for 15, 30, 60 minutes forecasting horizons as well as MAE, MSE, and MAPE averaged over a one-hour (12 steps) are reported. Best results are bold marked.

	PEMS03					PEMS04				
	15 min	30 min	60 min	Average		15 min	30 min	60 min	Average	
	MAE	MAE	MAE	MAE	MAPE (%)	MAE	MAE	MAE	MAE	MAPE (%)
AGCRN	14.65	15.72	16.82	15.58	15.08	18.27	18.95	19.83	18.90	12.69
DCRNN	14.59	15.76	18.18	15.90	15.74	19.19	20.54	23.55	20.75	14.32
Graph WaveNet	13.67	14.60	16.23	14.66	14.88	18.17	18.96	20.23	18.95	13.59
GatedGN	13.72	15.49	19.08	17.08	14.44	18.10	18.84	20.03	18.81	13.11
GRUGCN	14.63	16.44	19.87	16.62	15.96	19.89	22.28	27.37	22.68	15.81
EvolveGCN	17.07	19.03	22.22	19.11	18.61	23.21	25.82	30.97	26.21	17.79
ST-Transformer	14.03	15.72	18.74	15.85	15.37	19.13	21.33	25.69	21.63	15.12
STCN	14.27	15.49	18.02	15.61	16.07	19.26	20.75	24.03	20.95	14.79
STID	13.88	15.26	17.41	15.27	16.39	17.71	18.54	19.96	18.55	12.74
MTGNN	13.74	14.76	16.13	14.70	14.90	17.88	18.49	19.62	18.48	12.76
D2STGNN	13.36	14.45	15.96	14.45	14.55	17.60	18.39	19.63	18.39	12.65
DGCRN	14.34	15.54	17.53	15.52	15.20	18.05	18.76	20.07	18.77	13.13
DLinear	16.68	20.36	28.40	21.05	20.18	21.91	26.39	36.07	27.25	19.52
TimesNet	14.26	15.93	19.62	16.25	15.61	19.16	20.88	24.65	21.19	14.45
NexuSQN	13.26	14.27	15.82	14.25	14.12	17.48	18.20	19.37	18.19	12.58

Table 2: Results on benchmark traffic volume datasets. MAE for 15, 30, 60 minutes forecasting horizons as well as MAE and MAPE averaged over a one-hour (12 steps) are reported. Best results are bold marked.

processing based scalable predictor that encodes spatial-temporal features before model training. Similar to our work, Satorras et al. [22] developed a fully-connected gated GNN model (GatedGN) that effectively exploits the TTS format and global-local architecture. However, the all pairwise attention with time complexity $\mathcal{O}(n^2)$ is computationally very expensive. Along another line of research, a few methods are emerged to challenge the existing complicated models for LTSF problem, e.g., LightTS [11], LTSF-Linear [10], TS-Mixer [13], and TiDE [12]. Most of them belong to univariate models and do not contain explicit relational modeling.

As for positional encoding in STGNNs, Shao et al. [15] demonstrated that by concatenating both node and series PEs with the input data, MLPs could achieve competitive performances on several benchmark datasets. Cini et al. [17] further interpreted the role of node embedding as local effects and integrate it into a global-local architecture.

However, none of the existing works had thoroughly ex-

amined the essential model components for spatiotemporal forecasting directly, nor provided exhaustive discussions on the multiple roles of node identifications in STGNNs.

6 Empirical Evaluation

Extensive experiments are conducted to evaluate the performance of NexuSQN model on 8 well-known benchmark datasets and compare it with 14 baseline STGNN models. These datasets used in our evaluations vary from medium to large scale, covering traffic, energy, and air quality. All of the datasets are widely used benchmarks in modern time series analysis studies and the adopted baselines are selected from both state-of-the-art neural predictors, newly developed simple models, and classical STGNNs in the literature. Open-sourced implementations of NexuSQN as well as reproducible experiments are provided².

²Source code will be open-sourced upon publication

	PEMS07					PEMS08				
	15 min	30 min	60 min	Average		15 min	30 min	60 min	Average	
	MAE	MAE	MAE	MAE	MAPE (%)	MAE	MAE	MAE	MAE	MAPE (%)
AGCRN	19.55	20.65	22.40	20.64	9.42	14.50	15.16	16.41	15.23	10.46
DCRNN	20.47	22.11	25.77	22.30	9.51	14.84	15.93	18.22	16.06	10.40
Graph WaveNet	19.87	20.97	23.53	21.13	9.96	14.21	14.99	16.45	15.02	9.70
GatedGN	21.01	22.74	25.81	22.68	10.18	14.07	14.96	16.27	14.91	9.64
GRUGCN	21.15	24.00	29.91	24.37	10.29	15.46	17.32	21.16	17.55	11.43
EvolveGCN	24.72	28.09	34.41	28.40	12.11	18.21	20.46	24.45	20.64	13.11
ST-Transformer	20.17	22.80	27.74	23.05	9.77	14.39	15.87	18.69	16.00	10.71
STCN	20.26	22.33	26.58	22.53	9.66	14.81	16.02	18.76	16.20	10.57
STID	18.66	19.93	21.91	19.88	8.82	13.53	14.27	15.67	14.30	9.70
MTGNN	18.94	20.23	22.23	20.19	8.59	13.80	14.57	15.82	14.57	9.46
D2STGNN	-	-	-	-	-	13.65	14.53	16.00	14.52	9.40
DGCRN	-	-	-	-	-	13.96	14.68	15.96	14.70	9.62
DLinear	24.14	29.81	41.97	30.78	13.27	17.42	21.09	29.30	21.79	13.41
TimesNet	21.04	23.43	28.56	23.83	10.06	15.13	16.85	20.85	17.22	10.80
NexuSQN	18.50	19.78	21.72	19.74	8.26	13.38	14.19	15.50	14.20	9.26

Table 3: Results on benchmark traffic volume datasets. MAE for 15, 30, 60 minutes forecasting horizons as well as MAE and MAPE averaged over a one-hour (12 steps) are reported. Best results are bold marked.

6.1 EXPERIMENT SETUP

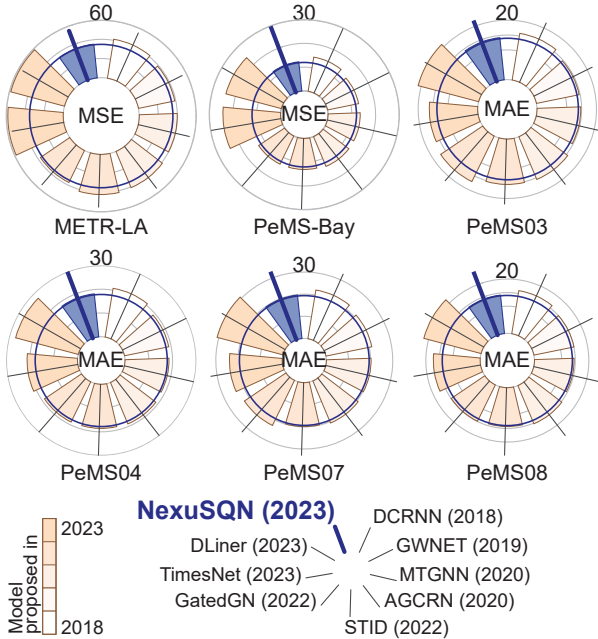


Figure 4: This figure compares the forecasting performance of our model, NexuSQN, with eight modern neural architectures on six well-known traffic benchmark datasets. Our model outperforms the others in all six datasets.

Datasets Six traffic flow datasets with high-resolution are used to compare the performances on short-term forecasting, including two traffic speed data: **METR-LA** and **PEMS-BAY** datasets [2], and four traffic volume data [51]: **PEMS03**, **PEMS04**, **PEMS07**, and **PEMS08**. All these traffic measurements are obtained from loop sensors in-

Table 4: Statistics of datasets used in the experiments.

DATASETS	Type	Steps	# of Nodes	# of Edges	Windows
METR-LA	traffic speed	34,272	207	1515	5 min
PEMS-BAY	traffic speed	52,128	325	2369	5 min
PEMS03	traffic volume	26,208	358	546	5 min
PEMS04	traffic volume	16,992	307	340	5 min
PEMS07	traffic volume	28,224	883	866	5 min
PEMS08	traffic volume	17,856	170	277	5 min
AQI	PM2.5 pollutant	8760	437	2699	60 min
PV-US	energy production	8868	5016	417199	30 min

stalled at highway networks and aggregated at 5 minutes. Then, we evaluate the scalability and the ability to forecast longer horizon on large-scale **PU-VS** production data which measures the energy production from farms in United States [52]. **AQI** data which reports the PM 2.5 pollutant collected by air quality monitoring stations spread across 43 Chinese cities [53] is adopted to evaluate models on data with high missing rate ($\approx 26\%$) and complex temporal patterns. Table 4 provides statistics about the studied datasets and detailed descriptions are given in appendix. In particular, all these benchmarks provide adjacent matrices constructed by the pairwise geographic distance between sensors as side information. The same graphs of previous works [3, 51, 31, 16] are prepared for baselines that require pre-defined graphs.

Baselines We consider a variety of deep learning baselines in the literature to benchmark our model: **AGCRN** [4]; **DCRNN** [2]; **Graph WaveNet** [3]; **GatedGN** [22]; **GRUGCN** [18]; **EvolveGCN** [54]; **ST-Transformer** [55]; **STCN** [1]; **STID** [15]; **MTGNN** [5]; **D2STGNN** [56]; **DGCRN** [57]; **DLinear** [10]; **TimesNet** [6]. To give a fair comparison and benchmark these methods, we use the official implementations in their original papers and use the recommended hyper-parameters on each dataset as far as possible. All baseline models are evaluated under the same training, validation, and testing environments.

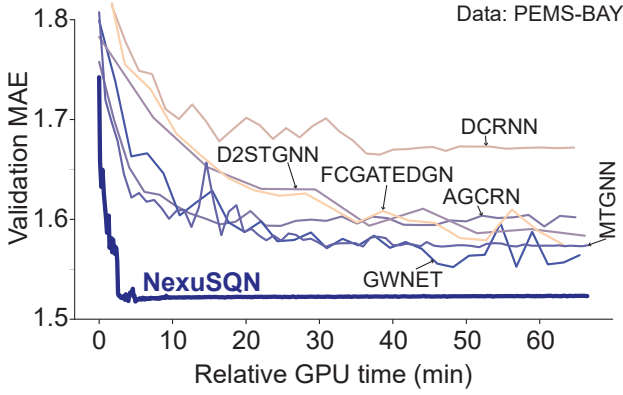


Figure 5: Validation MAE curves on PEMS-BAY traffic speed data. The x-axis represents the relative GPU running times of different models.

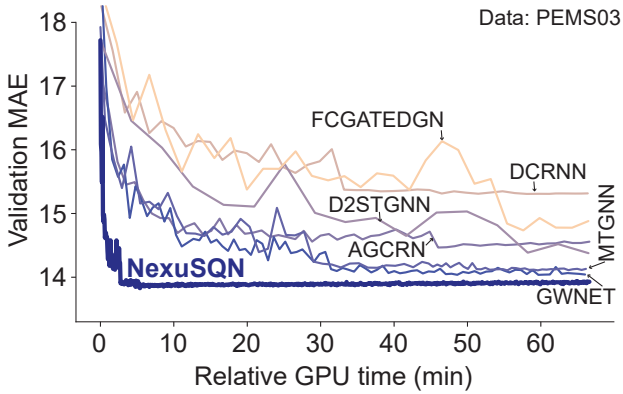


Figure 6: Validation MAE curves on PEMS03 traffic volume data. The x-axis represents the relative GPU running times of different models.

Experimental settings We follow the same experiment setups used in previous works wherever possible to provide unbiased evaluations. For six traffic benchmarks, we use 12-step historical values (1 hour) to forecast future 12-step observations (1 hour). For air quality data, we set the input window size as 24 steps (24 hours) and output size as 3 steps (3 hours). While for large-scale energy data, we adopt the settings in [16] that 36-steps are used as inputs and predictions at next {00 : 30, 07 : 30, 11 : 00} hours are used for evaluation. Quantitative metrics including *mean absolute error* (MAE), *mean squared error* (MSE), and *mean absolute percentage error* (MAPE) are calculated and reported.

6.2 EXPERIMENTAL RESULTS

Traffic benchmarks Model comparison results on six traffic flow benchmarks are displayed in Fig. 4. Detailed quantitative metrics are given in Tab. 1, 2 and 3. Intriguingly, our simple models have achieved comparable or even better performances than other complicated counterparts. In particular, forecasting METR-LA data is supposed to be more

challenging due to the complex temporal patterns of the observations, while our model consistently outperforms baselines by a large margin, even without any popular sequential techniques (Q1). As for PeMS-BAY data, the proposed model is still among the best-performing predictors. Notably, TimesNet and DLinear, which are proved to be powerful for LTSF, are less effective under the spatiotemporal setting. This may be due to a lack of spatial modeling. Compared with STID, our model features the extraction of distinguishable low-frequency node representations (Q3), thereby having better accuracy in all scenarios. Additionally, fully-attention based methods such as GatedGN, MTGNN, and D2STGNN also show competitive results. However, high memory requirements and computational complexities hinder them from large-scale applications (Q2).

Tab. 2 and 3 give the results on traffic volume records of different districts. Although our model does not depend on a pre-defined adjacent matrix, it still achieves the best performances. Different from loop speed, the distance-based correlation metrics may fail to describe the behavior of traffic volumes [38]. Our observation further confirms this claim. Kindly note that PeMS07 contains more than 8 hundreds of sensors so that the attention mechanism on the spatial dimension will lead to a prohibitive memory cost. Finally, although our model shares similar graph constructor with AGCRN, NexuSQN achieves more accurate predictions with conceptually more simpler procedure: constructs underlying graphs using PE directly (Q3).

Other benchmarks Tab. 5 reports the results on air quality and energy production benchmarks. Since PV-US contains more than 5 thousands nodes, several baselines are prone to be out-of-memory with limited GPU memory usage. It is worth commenting that there exists more dominating temporal patterns than spatial correlations in AQI data, hence baselines with advanced serial layers such as Graph WaveNet and D2STGNN can also achieve promising results. For large-scale problem like forecasting PV-US, stacking several sparse graph convolution operations can be neither cost-effective nor practical. What is noteworthy is that TimesNet, DLinear and STID produce desirable results without explicit spatial modeling. The residual connection enables our model to skip the graph aggregation flexibly when the graph information does not serve as an effective inductive basis. Moreover, two simple models with channel-dependence settings suffer from over-fitting problem and show poor performance in AQI data. On the contrary, we specialize the model parameter for each node with a learnable node identification, which introduces much fewer parameters than independent encoders (Q3).

Computational performance Apart from results on forecasting precision, we also examine the computational performance. Fig. 5 and 6 displays the validation MAE curves of several competing methods. Records of training speed and model size on METR-LA are exemplified in Fig. 1. Notably, NexuSQN enjoys a much faster training speed (converge in ten minutes of GPU time), smoother convergence curve, lower error bound. This indicates that our model is highly efficient and easy-to-train, requiring little manual interven-

	AQI					PV-US				
	1 hour	2 hour	3 hour	Average		30 min	7h 30 min	11 h	Average	
	MAE	MAE	MAE	MAE	MAPE (%)	MAE	MAE	MAE	MAE	MSE (%)
AGCRN	10.78	14.32	16.96	14.02	32.16	-	-	-	-	-
DCRNN	9.89	13.79	16.78	13.49	29.36	1.65	2.94	3.16	2.79	46.28
Graph WaveNet	9.39	12.98	15.71	12.70	28.31	1.48	6.13	7.66	4.86	149.75
GatedGN	10.39	14.68	17.76	14.28	32.45	-	-	-	-	-
GRUGCN	10.02	13.95	16.92	13.63	30.29	1.44	2.89	2.96	2.62	42.83
EvolveGCN	10.64	15.02	18.27	14.64	34.24	-	-	-	-	-
ST-Transformer	10.13	14.17	17.01	13.77	30.68	-	-	-	-	-
STCN	9.63	13.47	16.47	13.19	29.10	1.88	6.83	7.68	5.47	47.52
STID	10.44	14.76	17.88	14.36	32.97	1.42	2.67	2.76	2.45	41.10
MTGNN	10.24	14.10	16.83	13.72	29.42	1.81	3.11	3.14	2.96	48.18
D2STGNN	9.48	12.91	15.44	12.61	27.68	-	-	-	-	-
DGCRN	-	-	-	-	-	-	-	-	-	-
DLinear	10.99	15.79	19.31	15.36	37.09	1.59	3.11	3.08	3.27	60.48
TimesNet	17.64	19.47	21.10	19.40	47.19	1.47	2.75	2.80	2.51	39.99
NexuSQN	9.50	12.93	15.46	12.63	28.02	1.26	2.65	2.69	2.33	39.39

Table 5: Results on AQI and PV-US benchmarks. Note that - indicates the model runs out of memory with the minimum batch size. MAE for various forecasting horizons as well as average metrics are reported. Best results are bold marked.

tion and trick in the training stage. Such acceleration is achieved by the technically simple model architecture. Advanced STGNN approaches like DGCRN, D2STGNN apply a series of alternating graph convolution and autoregressive computations, resulting in a high computational burden and unstable optimization. Extra operations like self-attention or graph attention further complicate the process. In light of these results, it is worth commenting on the high efficiency of NexuSQN compared to other baselines.

7 Conclusion and Outlook

This work revisits the design of neural architectures for spatiotemporal forecasting of multivariate time series and demonstrate a conceptually and technically simple model, NexuSQN, to serve as an efficient, scalable, and powerful neural predictor. The success of NexuSQN builds on the concise architecture and versatility in the use of node embedding. Extensive and rigorous evaluations on several benchmarks indicate that NexuSQN not only outperforms a diverse array of baselines but also enjoys high computational efficiency. We believe that NexuSQN will constitute a scientific foundation for future research on the understanding and design of simpler neural forecasting architectures and helps the practitioners to develop more efficient tools in industrial applications. Future works include further exploring the performance on long-term series forecasting and wider variety of data, as well as the interpretability of NexuSQN.

Acknowledgements

This research was sponsored by the National Natural Science Foundation of China (52125208), and the Science and Technology Commission of Shanghai Municipality (No. 22dz1203200).

References

- [1] Bing Yu, Haoteng Yin, and Zhanxing Zhu. Spatio-temporal graph convolutional networks: a deep learning framework for traffic forecasting. In *Proceedings of the 27th International Joint Conference on Artificial Intelligence*, pages 3634–3640, 2018.
- [2] Yaguang Li, Rose Yu, Cyrus Shahabi, and Yan Liu. Diffusion convolutional recurrent neural network: Data-driven traffic forecasting. In *International Conference on Learning Representations*, 2018.
- [3] Zonghan Wu, Shirui Pan, Guodong Long, Jing Jiang, and Chengqi Zhang. Graph wavenet for deep spatial-temporal graph modeling. In *Proceedings of the 28th International Joint Conference on Artificial Intelligence*, pages 1907–1913, 2019.
- [4] Lei Bai, Lina Yao, Can Li, Xianzhi Wang, and Can Wang. Adaptive graph convolutional recurrent network for traffic forecasting. *Advances in neural information processing systems*, 33:17804–17815, 2020.
- [5] Zonghan Wu, Shirui Pan, Guodong Long, Jing Jiang, Xiaojun Chang, and Chengqi Zhang. Connecting the dots: Multivariate time series forecasting with graph neural networks. In *Proceedings of the 26th ACM SIGKDD International Conference on Knowledge Discovery and Data Mining*, page 753–763, New York, NY, USA, 2020. Association for Computing Machinery.
- [6] Haixu Wu, Tengge Hu, Yong Liu, Hang Zhou, Jianmin Wang, and Mingsheng Long. Timesnet: Temporal 2d-variation modeling for general time series analysis. *arXiv preprint arXiv:2210.02186*, 2022.
- [7] Haixu Wu, Hang Zhou, Mingsheng Long, and Jianmin Wang. Interpretable weather forecasting for worldwide stations with a unified deep model. *Nature Machine Intelligence*, pages 1–10, 2023.

- [8] Haoyi Zhou, Shanghang Zhang, Jieqi Peng, Shuai Zhang, Jianxin Li, Hui Xiong, and Wancai Zhang. Informer: Beyond efficient transformer for long sequence time-series forecasting. In *Proceedings of the AAAI conference on artificial intelligence*, volume 35, pages 11106–11115, 2021.
- [9] Minhao Liu, Ailing Zeng, Muxi Chen, Zhijian Xu, Qixia Lai, Lingna Ma, and Qiang Xu. Scinet: Time series modeling and forecasting with sample convolution and interaction. *Advances in Neural Information Processing Systems*, 35:5816–5828, 2022.
- [10] Ailing Zeng, Muxi Chen, Lei Zhang, and Qiang Xu. Are transformers effective for time series forecasting? *arXiv preprint arXiv:2205.13504*, 2022.
- [11] Tianping Zhang, Yizhuo Zhang, Wei Cao, Jiang Bian, Xiaohan Yi, Shun Zheng, and Jian Li. Less is more: Fast multivariate time series forecasting with light sampling-oriented mlp structures. *arXiv preprint arXiv:2207.01186*, 2022.
- [12] Abhimanyu Das, Weihao Kong, Andrew Leach, Rajat Sen, and Rose Yu. Long-term forecasting with tide: Time-series dense encoder. *arXiv preprint arXiv:2304.08424*, 2023.
- [13] Si-An Chen, Chun-Liang Li, Nate Yoder, Sercan O Arik, and Tomas Pfister. Tsmixer: An all-mlp architecture for time series forecasting. *arXiv preprint arXiv:2303.06053*, 2023.
- [14] Jianing Chen, Chuhao Chen, and Xiangxu Meng. Mlinear: Rethink the linear model for time-series forecasting. *arXiv preprint arXiv:2305.04800*, 2023.
- [15] Zezhi Shao, Zhao Zhang, Fei Wang, Wei Wei, and Yongjun Xu. Spatial-temporal identity: A simple yet effective baseline for multivariate time series forecasting. In *Proceedings of the 31st ACM International Conference on Information & Knowledge Management*, pages 4454–4458, 2022.
- [16] Andrea Cini, Ivan Marisca, Filippo Maria Bianchi, and Cesare Alippi. Scalable spatiotemporal graph neural networks. *arXiv preprint arXiv:2209.06520*, 2022.
- [17] Andrea Cini, Ivan Marisca, Daniele Zambon, and Cesare Alippi. Taming local effects in graph-based spatiotemporal forecasting. *arXiv preprint arXiv:2302.04071*, 2023.
- [18] Jianfei Gao and Bruno Ribeiro. On the equivalence between temporal and static equivariant graph representations. In *International Conference on Machine Learning*, pages 7052–7076. PMLR, 2022.
- [19] Andrea Cini, Daniele Zambon, and Cesare Alippi. Sparse graph learning for spatiotemporal time series. *arXiv preprint arXiv:2205.13492*, 2022.
- [20] Youngjoo Seo, Michaël Defferrard, Pierre Vandergheynst, and Xavier Bresson. Structured sequence modeling with graph convolutional recurrent networks. In *International Conference on Neural Information Processing*, pages 362–373. Springer, 2018.
- [21] Franco Manessi, Alessandro Rozza, and Mario Manzo. Dynamic graph convolutional networks. *Pattern Recognition*, 97:107000, 2020.
- [22] Victor Garcia Satorras, Syama Sundar Rangapuram, and Tim Januschowski. Multivariate time series forecasting with latent graph inference. *arXiv preprint arXiv:2203.03423*, 2022.
- [23] Justin Gilmer, Samuel S Schoenholz, Patrick F Riley, Oriol Vinyals, and George E Dahl. Neural message passing for quantum chemistry. In *International Conference on Machine Learning*, pages 1263–1272. PMLR, 2017.
- [24] Laura F Bringmann, Ellen L Hamaker, Daniel E Vigo, André Aubert, Denny Borsboom, and Francis Tuerlinckx. Changing dynamics: Time-varying autoregressive models using generalized additive modeling. *Psychological methods*, 22(3):409, 2017.
- [25] Pablo Montero-Manso and Rob J Hyndman. Principles and algorithms for forecasting groups of time series: Locality and globality. *International Journal of Forecasting*, 37(4):1632–1653, 2021.
- [26] Yuqi Nie, Nam H Nguyen, Phanwadee Sinthong, and Jayant Kalagnanam. A time series is worth 64 words: Long-term forecasting with transformers. *arXiv preprint arXiv:2211.14730*, 2022.
- [27] Rajat Sen, Hsiang-Fu Yu, and Inderjit S Dhillon. Think globally, act locally: A deep neural network approach to high-dimensional time series forecasting. *Advances in neural information processing systems*, 32, 2019.
- [28] Balasubramaniam Srinivasan and Bruno Ribeiro. On the equivalence between positional node embeddings and structural graph representations. *arXiv preprint arXiv:1910.00452*, 2019.
- [29] Ashish Vaswani, Noam Shazeer, Niki Parmar, Jakob Uszkoreit, Llion Jones, Aidan N Gomez, Łukasz Kaiser, and Illia Polosukhin. Attention is all you need. In *Advances in neural information processing systems*, pages 5998–6008, 2017.
- [30] Vijay Prakash Dwivedi, Chaitanya K Joshi, Thomas Laurent, Yoshua Bengio, and Xavier Bresson. Benchmarking graph neural networks. *arXiv preprint arXiv:2003.00982*, 2020.
- [31] Ivan Marisca, Andrea Cini, and Cesare Alippi. Learning to reconstruct missing data from spatiotemporal graphs with sparse observations. *arXiv preprint arXiv:2205.13479*, 2022.
- [32] Kaiming He, Xiangyu Zhang, Shaoqing Ren, and Jian Sun. Deep residual learning for image recognition. In *Proceedings of the IEEE conference on computer vision and pattern recognition*, pages 770–778, 2016.
- [33] Andreas Loukas. What graph neural networks cannot learn: depth vs width. *arXiv preprint arXiv:1907.03199*, 2019.
- [34] Vijay Prakash Dwivedi, Anh Tuan Luu, Thomas Laurent, Yoshua Bengio, and Xavier Bresson. Graph neural networks with learnable structural and positional

- representations. In *International Conference on Learning Representations*, 2022. URL <https://openreview.net/forum?id=wTTjnvGphYj>.
- [35] Jinliang Deng, Xiusi Chen, Renhe Jiang, Xuan Song, and Ivor W Tsang. St-norm: Spatial and temporal normalization for multi-variate time series forecasting. In *Proceedings of the 27th ACM SIGKDD conference on knowledge discovery & data mining*, pages 269–278, 2021.
- [36] Ryan Murphy, Balasubramaniam Srinivasan, Vinayak Rao, and Bruno Ribeiro. Relational pooling for graph representations. In *International Conference on Machine Learning*, pages 4663–4673. PMLR, 2019.
- [37] Hoang Nt and Takanori Maehara. Revisiting graph neural networks: All we have is low-pass filters. *arXiv preprint arXiv:1905.09550*, 2019.
- [38] Tong Nie, Guoyang Qin, Yunpeng Wang, and Jian Sun. Towards better traffic volume estimation: Tackling both underdetermined and non-equilibrium problems via a correlation adaptive graph convolution network. *arXiv preprint arXiv:2303.05660*, 2023.
- [39] Petar Veličković, Guillem Cucurull, Arantxa Casanova, Adriana Romero, Pietro Lio, and Yoshua Bengio. Graph attention networks. *arXiv preprint arXiv:1710.10903*, 2017.
- [40] Felix Wu, Amauri Souza, Tianyi Zhang, Christopher Fifty, Tao Yu, and Kilian Weinberger. Simplifying graph convolutional networks. In *International conference on machine learning*, pages 6861–6871. PMLR, 2019.
- [41] Chenxiao Yang, Qitian Wu, Jiahua Wang, and Junchi Yan. Graph neural networks are inherently good generalizers: Insights by bridging gnns and mlps. *arXiv preprint arXiv:2212.09034*, 2022.
- [42] Xiaotian Han, Tong Zhao, Yozen Liu, Xia Hu, and Neil Shah. Mlpinit: Embarrassingly simple gnn training acceleration with mlp initialization. *arXiv preprint arXiv:2210.00102*, 2022.
- [43] Taesung Kim, Jinhee Kim, Yunwon Tae, Cheonbok Park, Jang-Ho Choi, and Jaegul Choo. Reversible instance normalization for accurate time-series forecasting against distribution shift. In *International Conference on Learning Representations*, 2021.
- [44] Dmitry Ulyanov, Andrea Vedaldi, and Victor Lempit-sky. Instance normalization: The missing ingredient for fast stylization. *arXiv preprint arXiv:1607.08022*, 2016.
- [45] Qi Zhang, Jianlong Chang, Gaofeng Meng, Shiming Xiang, and Chunhong Pan. Spatio-temporal graph structure learning for traffic forecasting. In *Proceedings of the AAAI conference on artificial intelligence*, volume 34, pages 1177–1185, 2020.
- [46] Boris N Oreshkin, Arezou Amini, Lucy Coyle, and Mark Coates. Fc-gaga: Fully connected gated graph architecture for spatio-temporal traffic forecasting. In *Proceedings of the AAAI Conference on Artificial Intelligence*, volume 35, pages 9233–9241, 2021.
- [47] Aseem Baranwal, Kimon Fountoulakis, and Aukosh Jagannath. Effects of graph convolutions in multi-layer networks. In *The Eleventh International Conference on Learning Representations*, 2023.
- [48] Shengnan Guo, Youfang Lin, Ning Feng, Chao Song, and Huaiyu Wan. Attention based spatial-temporal graph convolutional networks for traffic flow forecasting. In *Proceedings of the AAAI Conference on Artificial Intelligence*, volume 33, pages 922–929, 2019.
- [49] Chuanpan Zheng, Xiaoliang Fan, Cheng Wang, and Jianzhong Qi. Gman: A graph multi-attention network for traffic prediction. In *Proceedings of the AAAI Conference on Artificial Intelligence*, volume 34, pages 1234–1241, 2020.
- [50] Zonghan Wu, Da Zheng, Shirui Pan, Quan Gan, Guodong Long, and George Karypis. Traversenet: Unifying space and time in message passing for traffic forecasting. *IEEE Transactions on Neural Networks and Learning Systems*, 2022.
- [51] Shengnan Guo, Youfang Lin, Huaiyu Wan, Xiucheng Li, and Gao Cong. Learning dynamics and heterogeneity of spatial-temporal graph data for traffic forecasting. *IEEE Transactions on Knowledge and Data Engineering*, 34(11):5415–5428, 2021.
- [52] Marissa Hummon, Eduardo Ibanez, Gregory Brinkman, and Debra Lew. Sub-hour solar data for power system modeling from static spatial variability analysis. Technical report, National Renewable Energy Lab.(NREL), Golden, CO (United States), 2012.
- [53] Yu Zheng, Xiuwen Yi, Ming Li, Ruiyuan Li, Zhangqing Shan, Eric Chang, and Tianrui Li. Forecasting fine-grained air quality based on big data. In *Proceedings of the 21th ACM SIGKDD international conference on knowledge discovery and data mining*, pages 2267–2276, 2015.
- [54] Aldo Pareja, Giacomo Domeniconi, Jie Chen, Tengfei Ma, Toyotaro Suzumura, Hiroki Kanezashi, Tim Kaler, Tao Schardl, and Charles Leiserson. Evolvegcn: Evolving graph convolutional networks for dynamic graphs. In *Proceedings of the AAAI conference on artificial intelligence*, volume 34, pages 5363–5370, 2020.
- [55] Mingxing Xu, Wenrui Dai, Chunmiao Liu, Xing Gao, Weiyao Lin, Guo-Jun Qi, and Hongkai Xiong. Spatial-temporal transformer networks for traffic flow forecasting. *arXiv preprint arXiv:2001.02908*, 2020.
- [56] Zezhi Shao, Zhao Zhang, Wei Wei, Fei Wang, Yongjun Xu, Xin Cao, and Christian S Jensen. Decoupled dynamic spatial-temporal graph neural network for traffic forecasting. *arXiv preprint arXiv:2206.09112*, 2022.
- [57] Fuxian Li, Jie Feng, Huan Yan, Guangyin Jin, Fan Yang, Funing Sun, Depeng Jin, and Yong Li. Dynamic graph convolutional recurrent network for traffic prediction: Benchmark and solution. *ACM Transactions on Knowledge Discovery from Data*, 17(1):1–21, 2023.